

## PDF hosted at the Radboud Repository of the Radboud University Nijmegen

The following full text is a publisher's version.

For additional information about this publication click this link.

<http://hdl.handle.net/2066/112786>

Please be advised that this information was generated on 2018-07-08 and may be subject to change.

# OPTICAL EMISSION AND RAMAN SCATTERING IN MODULATION-DOPED GaAs-AlGaAs QUANTUM WIRES AND DOTS

P.D. Wang, Y.P. Song, C.M. Sotomayor Torres\* and M.C. Holland

Nanoelectronics Research Centre, Department of Electronics and Electrical Engineering,  
University of Glasgow, Glasgow G12 8QQ, UK

D.J. Lockwood, P. Hawrylak and J.J. Palacios†

Institute of Microstructural Sciences, National Research Council, Ottawa, Canada K1A 0R6

P.C.M. Christianen, J.C. Maan and J.A.A.J. Perenboom

High Field Magnet Laboratory and Research Institute for Materials, University of Nijmegen,  
Toernooiveld, 6525 ED Nijmegen, The Netherlands

(Received 22 August 1994)

Magneto-optical properties and resonant Raman spectroscopy of modulation doped GaAs-AlGaAs quantum well wires are reported. Their properties are compared with similar undoped quantum well wires to investigate the many electron effects in nanostructures. In undoped samples, the quantised energy levels observed by luminescence excitation spectroscopy are in good agreement with a particle-in-a-box model. In doped samples, the carrier confinement is explicitly revealed by magnetoluminescence and depolarised resonant Raman scattering. The calculated spectra in a Hartree model are in reasonable agreement with experiment.

PACS: 78.66.Fd, 78.30.Fs, 78.55.Cr, 73.20.Dx

Keywords: Raman scattering; magnetoluminescence; GaAs-AlGaAs; wires and dots.

The realization of semiconductor nanostructures, such as quantum wires and dots, has been achieved mainly through advances in in-situ epitaxial growth and in nanometer scale lithography. New features such as energy quantization and enhanced exciton binding induced by the quantum confinement effects have been reported<sup>1-6</sup> based upon photoluminescence (PL), photoluminescence excitation (PLE) and electroluminescence studies. The carrier energy and momentum relaxation dependence on the dimensions and length scale of the nanostructures have also attracted much attention mainly due to their impact on the potential use for opto-electronic devices<sup>7,8</sup>.

In this paper, we report on the optical emission properties and resonant Raman scattering of undoped and modulation doped semiconductor quantum wires and dots of width down to 60 nm. The magneto-photoluminescence and Raman spectra of modulation doped samples are compared with the undoped samples to investigate the many electron effects in nanostructures. The presence of many electrons modifies the electronic properties of

nanostructures. The form of the confining potential, including the effect of a depletion layer and possible traps, the donor charge distribution, and Hartree and exchange correlation contribution from electron-electron interactions are the most important effects determining the ground state charge density and excitation spectrum. The many electron effects manifest themselves in the photoluminescence and absorption spectrum in terms of bandgap renormalization<sup>9,10</sup> (electron and valence hole self-energy), in the form of the Fermi edge singularity (many-electron excitonic effects)<sup>11</sup> and as shifts in the charge density excitations (CDE), single particle excitations (SPE) and spin density excitations (SDE)<sup>12-14</sup>. The SPE corresponds to transitions between filled and empty quantum levels. The SDE energy is lowered from the SPE energy due to the attractive interaction of an excited electron with the hole left in the ground state (excitonic shift). The energy of the CDE is a competition between the excitonic red shift and the depolarization blue shift. The depolarization shift is simply an ability of electrons to screen the applied field by modifying their charge density and, hence, their Hartree fields<sup>15</sup>. The effect of the depolarization and excitonic shifts can be measured from a comparison of the CDE, SPE, and SDE energies. As a first step in this direction, the magneto-PL and Raman scattering spectra have been modeled using a

\* Royal Society of Edinburgh Research Fellow

† Departamento de Física de la Materia Condensada, Universidad Autónoma de Madrid, Cantoblanco, 28049, Madrid, Spain

Hartree approximation without excitonic effects. The calculated results show a reasonable agreement with the experiment and are a good starting point for more sophisticated calculations now in progress.

The modulation doped quantum well structure (sample B) was grown by solid source molecular beam epitaxy on a (001) semi-insulating GaAs substrate with a 1  $\mu\text{m}$  unintentionally doped GaAs buffer. The active region was a 580 nm thick multiple quantum well (MQW) structure, which consisted of the following layers repeated 10 times: a 30 nm  $\text{Al}_{0.3}\text{Ga}_{0.7}\text{As}$  layer, a  $\delta$ -doped layer ( $2 \times 10^{12} \text{ cm}^{-2}$ ), 20 nm of a  $\text{GaAs}(0.85 \text{ nm})/\text{AlAs}(0.85 \text{ nm})$  superlattice structure, and a 8 nm GaAs quantum well region. There was a 17 nm GaAs cap on top of the entire structure. Shubnikov-de Haas measurements at 4 K indicated a two dimensional electron carrier concentration of  $8.5 \times 10^{11} \text{ cm}^{-2}$  and a mobility of  $2.85 \times 10^4 \text{ cm}^2/\text{V}\cdot\text{s}$ . Considering the rather narrow quantum well width (8 nm) and the high carrier concentration, the sample is of high quality. The asymmetric barrier growth pattern was adopted to compensate the different properties of MBE-grown GaAs/AlAs and AlAs/GaAs interfaces, and was shown to produce a more symmetric well potential profile. This was confirmed by the Shubnikov-de Haas measurements. The undoped sample (sample A) has similar buffer structures. The active region consists of a 30-period 12 nm  $\text{Al}_{0.3}\text{Ga}_{0.7}\text{As}/8 \text{ nm}$  GaAs MQW structure. The cap layer is 10 nm of GaAs.

Patterns were defined by electron beam lithography (Leica Cambridge EPBG 5HR electron beam machine working at 50 keV) using a standard double layer PMMA resist. After the development of the resist, a 30 nm layer of NiCr was deposited before the lift-off and subsequently used as an etching mask. The smallest structure achieved routinely is  $\sim 30 \text{ nm}$  diameter dots and wires. For pattern transfer, a low damage, anisotropic, reactive ion etching process has been developed using  $\text{SiCl}_4$ <sup>16</sup>. Using low radio frequency power of 30 W, and hence low DC bias of 70 V, pressure of 8 mTorr and the flow rates of 6 sccm, the damage was kept to a minimum value while maintaining very good anisotropy with an aspect ratio of  $>10:1$ . The very low etching damage in both surface and sidewalls was determined by conductivity<sup>17</sup> and Raman scattering techniques<sup>18</sup>. The etching rate was 150 nm/min. The etch depth was usually 700 nm so that all the quantum wells were etched through.

Figure 1(a) shows the photoluminescence excitation spectra of sample A (undoped quantum wells) and  $W = 60 \text{ nm}$  quantum well wires (QWW). Heavy hole and light hole exciton states were readily observed. In 60 nm QWW, exciton states associated with three 1D subbands were also observed with an energy separation of  $\sim 4 \text{ meV}$ . Such energy separations are also in agreement with the centre-of-mass quantizations<sup>1</sup> with  $m=1, 3$  and 5. However, the linear polarisation spectra did not show  $m = 2$  exciton centre-mass motion and the subband transitions

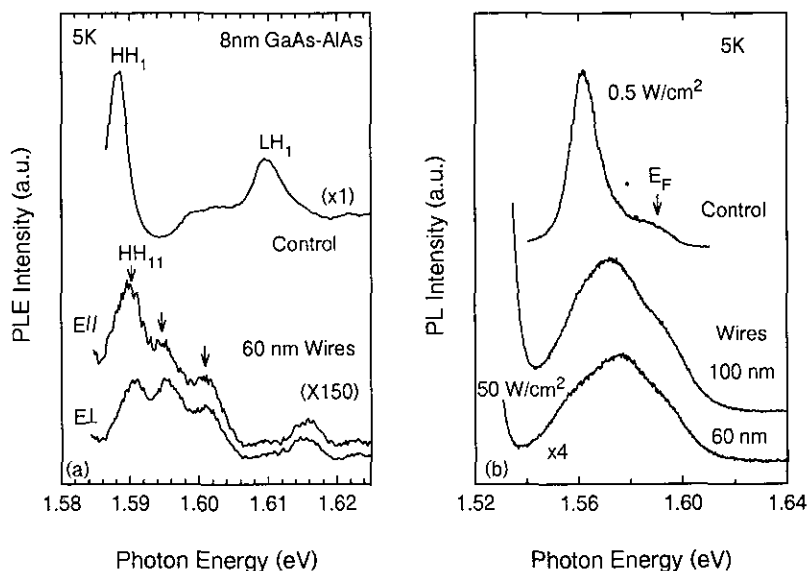


Fig. 1.

(a) The 5 K PLE spectra of an undoped 8 nm GaAs quantum well and  $W = 60 \text{ nm}$  quantum well wires. E// and E $\perp$  indicate that the excitation electric field is parallel and perpendicular to the wire length, respectively. (b) The 5 K PL spectra of the GaAs modulation doped quantum well (control sample), 100 nm and 60 nm multiple quantum well wires. The excitation line is 514.5 nm from an  $\text{Ar}^+$  laser.

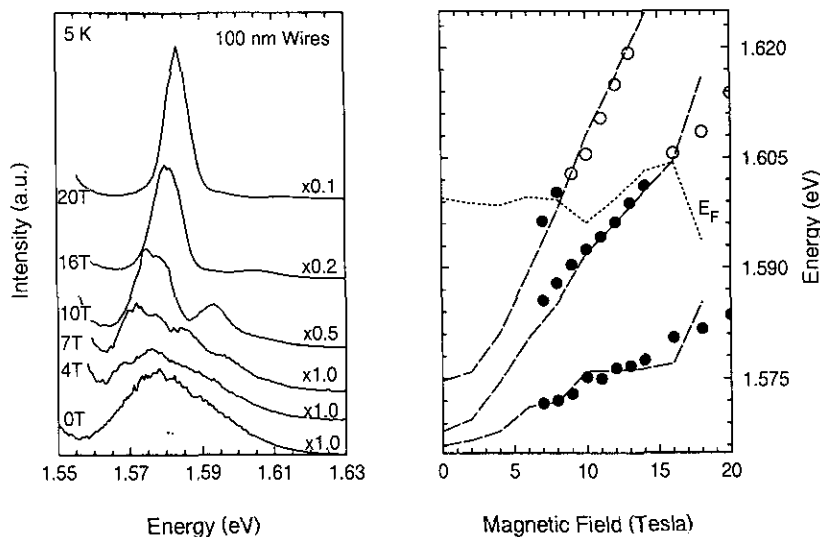


Fig. 2.

(a) The magneto-PL spectra and (b) the fan-chart diagram of  $W = 100$  nm modulation doped quantum well wires. Dashed lines correspond to the theoretical curves discussed in the text. The empty circles indicate the depopulation of free carriers and correspond to a decrease of luminescence intensity.

are more likely due to 1D quantum confinement. Figure 1(b) shows the PL spectra of the control part of sample B (unpatterned),  $W = 100$  nm and 60 nm modulation doped QWW. The spectra are very broad and the effect of lateral quantization in the density of states (QWW subband structure) is not visible, but an overall blue shift of the mean energy of the emission line is evident in 60 nm and 100 nm wires. Such a broad spectral line may result from inhomogeneities in individual wire widths and from averaging over an ensemble of different wires<sup>5</sup>. The width of the spectral line, which is difficult to relate to the Fermi energy, puts in question the presence of free carriers in the wires. In order to identify free carriers and to observe clear lateral quantum confinement effects, magnetic fields of up to 20 Tesla were applied to 100 nm and 60 nm wires. Figure 2 shows the magneto-PL spectra of 100 nm wires and its fan-chart diagram. The QWW subband energies evolve from the quantization imposed by the external effective confining potential to the usual Landau quantization in the magnetic field. We were able to identify clearly up to three populated QWW subbands for  $B > 7$  T. By extrapolating to  $B = 0$  T, we find a subband spacing of approximately  $E_{01} = 2$  meV and  $E_{02} = 10$  meV. The very small energy spacing of the symmetric-antisymmetric gap and a large spacing of the third subband is indicative of a net repulsive potential in the center of the wire due to electron-electron repulsion. With increasing magnetic field, QWW subbands depopulate. The depopulation of subbands leads to changes in the lateral charge distribution and Hartree potentials and subband energies. These changes are evident through shifts in the positions of recombination line from populated subbands when the highest energy subband

depopulates. We calculated subband energies in the Hartree approximation for an effective wire width of  $W = 60$  nm, infinite square well confining potential, 2D carrier density  $n = 8.5 \times 10^{11} \text{ cm}^{-2}$ , and a positive charge distribution of donors at a distance  $D = 20$  nm from the wire along the growth direction. The electron subband energies and the Fermi level are shown in Fig. 2(b) (dashed lines) together with experimental data (circles). We find good overall agreement between calculated and measured subband spacing, and shifts in the position associated with subband depopulation. In undoped quantum well wires, a particle-in-a-box model gives a lowest subband spacing of  $\sim 4$  meV in 60 nm wires, again in good agreement with the PLE spectra (Fig. 1(a)). The above comparisons demonstrate clearly the many electron effects in 1D quantum well wires.

The structure in the emission of the unpatterned 2D electron gas associated with depopulation of Landau levels at even filling factors are well known and are due predominantly to oscillations of the valence hole self-energy<sup>19</sup>. We find theoretically that for an 8 nm quantum well, the heavy hole in the lowest subband  $HH_1$  has a very large in-plane mass ( $m_h = 12m_e$ ), thereby reducing the possibility that the observed structures are due to the valence hole self-energy. Both the magnetic field dependence of QWW energy levels and structures associated with subband depopulation indicate clearly both the lateral quantization of electronic motion and the presence of free carriers in our wires. From the reasonable agreement between calculations and magneto-PL an effective wire width of approximately 60 nm for the 100 nm wire sample is deduced.

Resonant Raman scattering shows clearly the 1D-

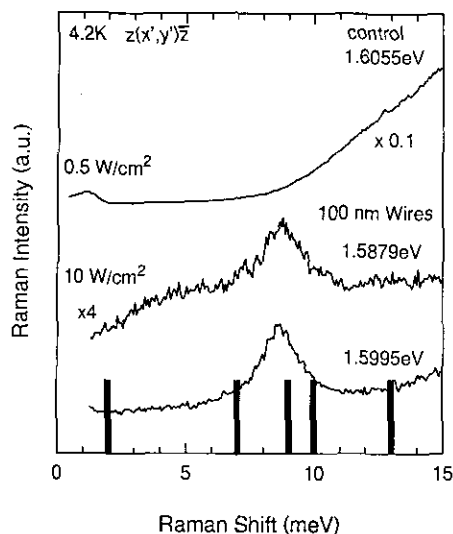


Fig. 3. Depolarized resonant Raman spectra (bottom two curves) of 100 nm modulation doped quantum well wires under different excitation energies. The top curve shows the depolarised Raman spectra of the control sample. A peak at 1.5 meV is observed and corresponds to the SPE-like excitations.  $x'$ ,  $y'$  and  $z$  denote  $[110]$ ,  $[1\bar{1}0]$  and  $[001]$  crystal directions, respectively. The vertical bars are the calculated Hartree subband spacings.

intersubband SDE excitations in modulation doped GaAs quantum wires. SDE energies correspond to a good approximation to energies of transitions from populated to empty 1D subbands, shifted by the excitonic effects. Figure 3 shows the SDE Raman spectra of 100 nm wires for two different near resonance energies. There is a strong feature at approximately 8.5 meV and a weak feature at approximately 3-4 meV. The weak feature is most sensitive to the excitation energy. As bars, we show calculated Hartree subband spacings for a 60 nm wire, discussed previously in the context of PL. For five occupied subbands we find the lowest energy transition at approximately 2 meV and other transitions at 7, 9, 10 and 13 meV. The calculated energy of the lowest transition at 2 meV is lower from the measured transition by 1-2 meV, but a group of transitions around 9 meV coincides nicely with the strong experimental peak at 8.5 meV. Since actual transition energies are different from Hartree transition energies due to exchange-correlation and finite state interaction (excitonic) effects<sup>20</sup>, the agreement observed here may very well be superficial. However, an overall qualitative agreement between calculated energies in magneto-PL and Raman scattering is encouraging. Similarly, in 60 nm wires, a weak Raman peak at 4.5 meV and a strong peak at 11.5 meV were observed. These results are again consistent with the magneto-PL observed for that sample.

Raman scattering from 100 nm quantum dots was also investigated. Figure 4 shows different subband

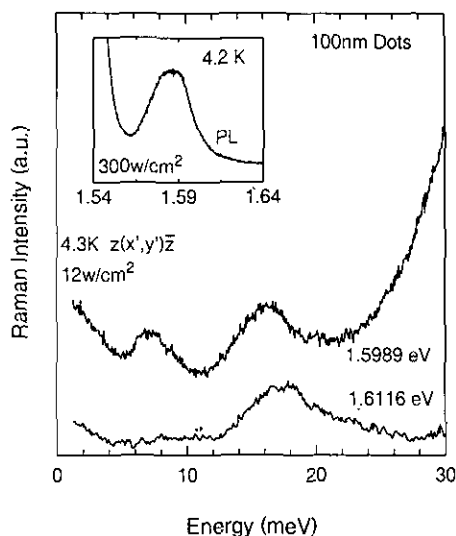


Fig. 4. Depolarization electronic Raman scattering from 100 nm quantum dots at 4.3 K using different excitation energies. The inset shows the PL spectrum at 4.2 K.

transitions in the regions of 8 meV and 17 meV. With fine tuning of the excitation energy, we can observe several different peaks around 17 meV, indicating different intersubband transitions related to lateral confinement. The PL blue shift (see Fig. 4) for this sample is consistent with the Hartree field calculations for 60 nm dots, much as was found for the wires.

In conclusion, we have performed magneto-luminescence and resonant Raman studies in quantum well wires and dots. The magneto-PL and resonant Raman showed spectral features identified with the presence of free carriers and with effects of lateral quantization on the energy spectrum. We have demonstrated that resonant Raman scattering can be effectively used to probe the lateral quantum confinement in quantum well wires and dots.

**Acknowledgement** -The authors thank the EPSRC (UK) (Grant No: GR/J90718) and European Community (Grant No: ESPRIT Project QUANTECS 6312) for financial support.

## REFERENCES

1. D. Heitmann, H. Lage, M. Kohl, R. Cingolani, P. Grambow, and K. Ploog, *Inst. Phys. Conf. Ser.* **123**, 109 (1992); M. Kohl, D. Heitmann, P. Grambow and K. Ploog, *Phys. Rev. Lett.* **63**, 2124 (1989)
2. H. Temkin, G.J. Dolan, M.B. Panish, and S.N.G. Chu, *Appl. Phys. Lett.* **50**, 413 (1987)
3. K. Brunner, U. Bockelmann, G. Abstreiter, M. Walter, G. Böhm, G. Tränkle and G. Weimann, *Phys. Rev. Lett.* **69**, 3216 (1992)
4. P.D. Wang and C.M. Sotomayor Torres, *J. Appl. Phys.* **74**, 5052 (1993)

5. M. Fritze, A.V. Nurmikko and P. Hawrylak, Phys. Rev. B **48**, 4960 (1993)
6. G. Gumbs, D. Huang, H. Qiang, F.H. Pollak, P.D. Wang, C.M. Sotomayor Torres and M.C. Holland, to be published in Phys. Rev. B (1994)
7. H. Benisty, C.M. Sotomayor Torres, and C. Weisbuch, Phys. Rev. B **44**, 10945 (1991), also P.D. Wang, C.M. Sotomayor Torres, H. Benisty and C. Weisbuch, Appl. Phys. Lett. **61**, 946 (1992)
8. U. Bockelmann and G. Bastard, Phys. Rev. B **42**, 8947 (1990)
9. D.A. Kleinman and R.C. Miller, Phys. Rev. B **32**, 2266 (1985)
10. S. Haacke, R. Zimmermann, D. Bimberg, H. Kal, D.E. Mars and J.N. Miller, Phys. Rev. B **45**, 1737 (1992)
11. M.S. Skolnick, J.M. Rorison, K.J. Nash, D.J. Mowbray, P.R. Tapster, S.J. Bass and A.D. Pitt, Phys. Rev. Lett. **58**, 2130 (1987)
12. A. Pinczuk and G. Abstreiter in *Light Scattering in Solids V*, Eds: M. Cardona and G. Güntherodt (Springer, Berlin), 153 (1989)
13. A.R. Goñi, A. Pinczuk, J.S. Weiner, J.M. Calleja, B.S. Dennis, L.N. Pfeiffer, and K. West, Phys. Rev. Lett. **67**, 3298 (1991)
14. G. Eliasson, P. Hawrylak and J.J. Quinn, Phys. Rev. B **35**, 5569 (1987)
15. P. Hawrylak, Phys. Rev. Lett. **71**, 3347 (1993); P. Hawrylak, unpublished (1994)
16. Y.P. Song, P.D. Wang, C.M. Sotomayor Torres and C.D.W. Wilkinson, to be published in J. Vac. Sci. Technol. B (1994)
17. S.K. Murad, C.D.W. Wilkinson, P.D. Wang, W. Parkes, C.M. Sotomayor Torres, and N. Cameron, J. Vac. Sci. Technol. B **11**, 2237 (1993)
18. P.D. Wang, M.A. Foad, C.M. Sotomayor Torres S. Thoms, M. Watt, R. Cheung, C.D.W. Wilkinson, and S.P. Beaumont, J. Appl. Phys. **71**, 3754 (1992)
19. T. Uenoyama and L.J. Sham, Phys. Rev. B **39**, 11044 (1989)
20. R. Decca, A. Pinczuk, S. Das Sarma, B.S. Dennis, L.N. Pfeiffer and K.W. West, Phys. Rev. Lett. **72**, 1506 (1994)